Mechanism of Thermal Runaway in Lithium-Ion Cells

N. E. Galushkin, *,z **N. N. Yazvinskaya, and D. N. Galushkin**

Don State Technical University, Laboratory of Electrochemical and Hydrogen Energy, Town of Shakhty, Rostov Region 346500, Russia

In this investigation, it was shown that a probability of thermal runaway in commercial lithium-ion cells of the type 18650 grows with number increase of charge/discharge cycles and increase of cells state of charge (SOC). Notably, experiments in an accelerating rate calorimeter (ARC) showed that with the number growth of cells charge/discharge cycles, it is observed a considerable decline of an initiation temperature of exothermic reactions of thermal runaway and increase of released energy. Additional ARC-experiments with the following analysis of the gas released showed that in a course of cells cycling in anode graphite, hydrogen is accumulated. It was proven in experiments that a recombination of released-from-graphite-anode atomic hydrogen is exactly that powerful exothermic reaction, which increases the released energy in the beginning of the thermal runaway and decreases the temperature of its initiation. Thus, the reason for the initiation of thermal runaway in lithium-ion cells is a powerful exothermic reaction of recombination of atomic hydrogen accumulated in anode graphite in a during of cells cycling. The possible mechanism of initiation thermal runaway has been proposed corresponding to all the experimental results obtained.

 [DOI: 10.1149/2.0611807jes]

Manuscript submitted February 14, 2018; revised manuscript received March 28, 2018. Published May 2, 2018.

At present, lithium-ion batteries are ones of the most promising electrochemical systems of energy storing. They are dominant energy sources in hand-hold devices: smartphones, notebooks, tablets, etc.[1] In more recent times more and more extensively, the lithium-ion batteries started finding use in the segment of high capacity batteries, primarily for electric vehicles (xEV) as well as for aviation.[2–5] The widespread prevalence of the lithium-ion batteries is connected with high specific parameters of their capacity and power as well as with their long term operation. Nevertheless, in common with batteries of other electrochemical systems, these batteries are subjected to the thermal runaway phenomenon. In a case of the thermal runaway initiation, a battery heats up sharply, gets on fire and can even explode. To investigation of the thermal runaway phenomenon in lithium-ion batteries, a great deal of papers is devoted.[2–7] It is thought that the thermal runaway is connected with occurrence of a variety of exothermic reactions in batteries. According to generally accepted point of view,[8] at a battery heating up, the first exothermic reaction is the reaction of SEI layer decomposition (80–120°C) with a subsequent interaction between anode lithium and electrolyte.[8,9] In a course of further battery heating up, even more powerful exothermic reactions occur connected with oxygen release from a cathode and its interaction with the electrolyte.[10,11] There are no doubts in a possibility of such exothermic reactions existence. However, in our humble opinion, an impact of aging processes on those exothermic reactions is investigated not enough. As a matter of fact, the aging processes in lithium-ion cells were investigated in many papers.[12–14] Nevertheless, there exist rather few combined researches in the area of the processes of the thermal runaway and the aging.[15–17] Besides, as it was highlighted in the paper,[17] in main, the combined researches focused on influence of aging parameters on cells operation safety without a clarification of mechanisms and underlying causes.

In this paper, influence is investigated of aging processes of lithium-ion cells on a probability of a thermal runaway occurrence.

Experimental

On aging processes of lithium-ion cells, virtually all factors influence, in presence of which cells are operated including as follows: cells charge/discharge modes, temperature, cell design, cell chemistry, etc.[13,14,18,19] One of the most important mechanisms of aging is considered to be the process of metal lithium deposition on an anode.[20,21] The metal lithium deposition is intensified at decrease of temperature of cells cycling down to T = 0°C.[22–24] That is why we cycled cells in the climatic chamber Binder MK240 (BINDER GmbH, Germany) at the temperature T = 0°C, which accelerates aging processes dramatically.[17]

In this research, there were used the commercial lithium-ion cells with geometrical format 18650 (2.2 Ah, $Li(Ni_{0.5}Co_{0.2}Mn_{0.3})O_2$/Graphite), i.e. cells (NCM/Graphite). In order to investigate these cells with due consideration of their diverse operating life, they were cycled according to the following protocol. The charging procedure consisted in use of constant current/constant voltage (CC/CV). The charging current was 1C (2.2 A) up to voltage 4.2 V. Then the charge grew at the constant voltage 4.2 V until the charging current decreased lower than C/20. The discharging procedure consisted in use of constant current (CC). The discharging current was 1C (2.2 A) and it was used until the voltage on cell terminals reached 2.75 V.

For obtaining of a considerable amount of statistical material within a short period of time, ten parallel connected cells were cycled at the same time. During cycling, the cells were situated in the distance of 5 cm from each other, in order to exclude a mutual thermal heating up, which could make impact on a probability of thermal runaway occurrence. The average change of discharge capacity for these cells is shown in the Fig. 1.

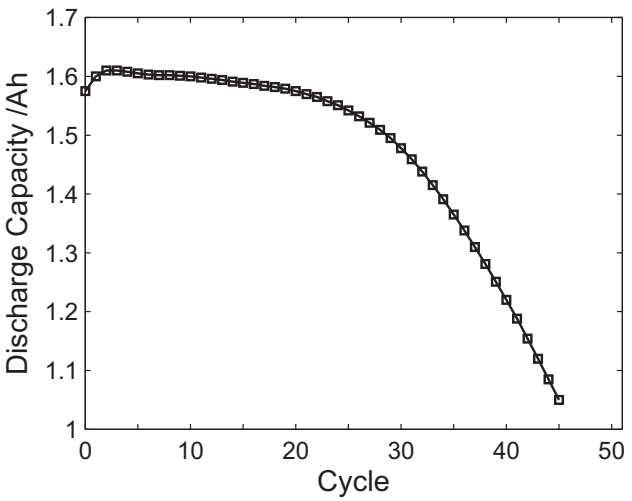

Figure 1. Mean change of discharge capacity of ten cells during their cycling at the temperature 0°C.

*Electrochemical Society Member.
zE-mail: galushkinne@mail.ru

For the investigation, four groups of cells were prepared with number of cycles (NC) of charge/discharge 0, 15, 30 and 45 respectively. According to cells cycling results (Fig. 1), after 45 cycles of charge/discharge (at T = 0°C), their discharge capacity fell down to 70% of their initial discharge capacity, i.e. of the discharge capacity of the first cycle. It should be noted that the initial discharge capacity of the cells is much lower of their nominal capacity as cycling took place at low temperatures and hence at higher resistance of the cells. Usually, the decrease of the cells discharge capacity down to 70% of their initial discharge capacity is considered to be the end of cells lifetime.[25,26]

For determining of lifetime influence of the cells 18650 (NCM/Graphite) to a probability of a thermal runaway occurrence, there were performed sessions of calorimetric measuring with use of the accelerating rate calorimeter (ARC) in the mode of heat-wait-search (HWS) at quasi-adiabatic conditions. In the experiments, there was used the Extended Volume Accelerating Rate Calorimeter (EV-ARC) made by Thermal Hazard Technology (THT, UK). By experiments, there were examined four groups of cells with the following numbers of charge/discharge cycles (NC): 0, 15, 30 and 45. For ARC-calorimetric measuring, the following parameters were used: Heat Steps ΔT = 5 K, Wait Time 30 minutes, Detection Sensitivity of an exothermic reaction (DSER) 0.02 K min^{-1}. When speed of cell temperature growth exceeds the selected sensitivity (DSER), automatically, the system switches over to the Exotherm mode and follows in tracks of changes of cell surface temperature, while measuring parameters of an occurred exothermic reaction. Based on preliminary experiments with the four above specified groups of cells, the initial temperature for ARC calorimetric measuring was selected as follows: 70°C, 68°C, 46°C and 27°C respectively. In order to ensure a data reproducibility, the entire measuring was conducted not less than three times. Besides, for every group of cells, measuring was conducted at the following states of charge (SOC): 0%, 50% and 100%. The experimental results are represented in Fig. 2.

In the course of the experiment for different groups of cells and SOC, there were measured parameters most characteristic for cells Self-Heating Rate (SHR), namely: temperature of initiation of the exothermic reactions (at SHR = 0.02 K min^{-1}), temperature of thermal runaway at SHR = 0.2 K min^{-1} and temperature of the current interrupt device activation (Fig. 3).

Results and Discussion

In the paper,[17] results of ARC calorimetric measuring for cells 18650 (NCM/Graphite) are analyzed. The whole process of a thermal runaway (Fig. 2) was divided by authors in three stages. Each of the stages is generated by different groups of exothermic reactions.

The first group of the exothermic reactions creates the first maximum on the curves of the Fig. 2 (NC = 45,30,15) at any values of SOC. This group of the exothermic reactions takes place approximately in the temperature range from the temperature of exothermic reactions initiation $T_{DSER} \approx 32$°C (for cells with NC = 45, Fig. 2) till the temperature of the first maximum $T_{max} \approx 116$°C (Fig. 2).

The second group of the exothermic reactions takes place approximately in the temperature range from the temperature of exothermic reactions initiation $T_{DSER} \approx 90$–125°C (for cells with NC = 0 (Fig. 2) at various SOC) till the temperature of oxygen release start on a cathode, which is equal approximately $T_{ox} \approx 200$–250°C (Fig. 2). This group of exothermic reactions is investigated quite well.[11,27,28] It is resulting from a degradation of the layer SEI with a subsequent de-intercalation of lithium ions on graphite surface. In a case of sufficient amount of lithium in anode, the damaged layer SEI can be recovered permanently on expense of electrolyte reduction. This process is exothermic and it will continue as long as there is lithium in the anode.[11,27,28]

The third group of the exothermic reactions proceeds in the temperature range from beginning of oxygen release from a cathode, approximately at $T_{ox} \approx 200$–250°C till the end of the thermal runaway process (Figs. 2). In this temperature range, a cathode thermal decomposition is accompanied with release of oxygen, which reacts afterwards with electrolyte.[29,30] The exothermic reactions of electrolyte burning on a cathode are dominant in the course of the thermal runaway of lithium-ion cells.[5] From Figs. 2b, 2c, it is seen that with growth of SOC, the temperature of the thermal runaway shifts to the side of lower values. This is connected with the fact that with the SOC growth, a cathode thermal stability falls, while oxygen release from a cathode grows.[5,29] This group of exothermic reactions is well investigated, too.

The first group of the exothermic reactions proceeding in the beginning of the thermal runaway in cells (Fig. 2) is investigated extremely scanty. In the paper,[17] the authors suppose that these exothermic reactions are connected with processes of thermal degradation of electrolyte (based on EC/DMC) in contact with an anode (LiC_6). The

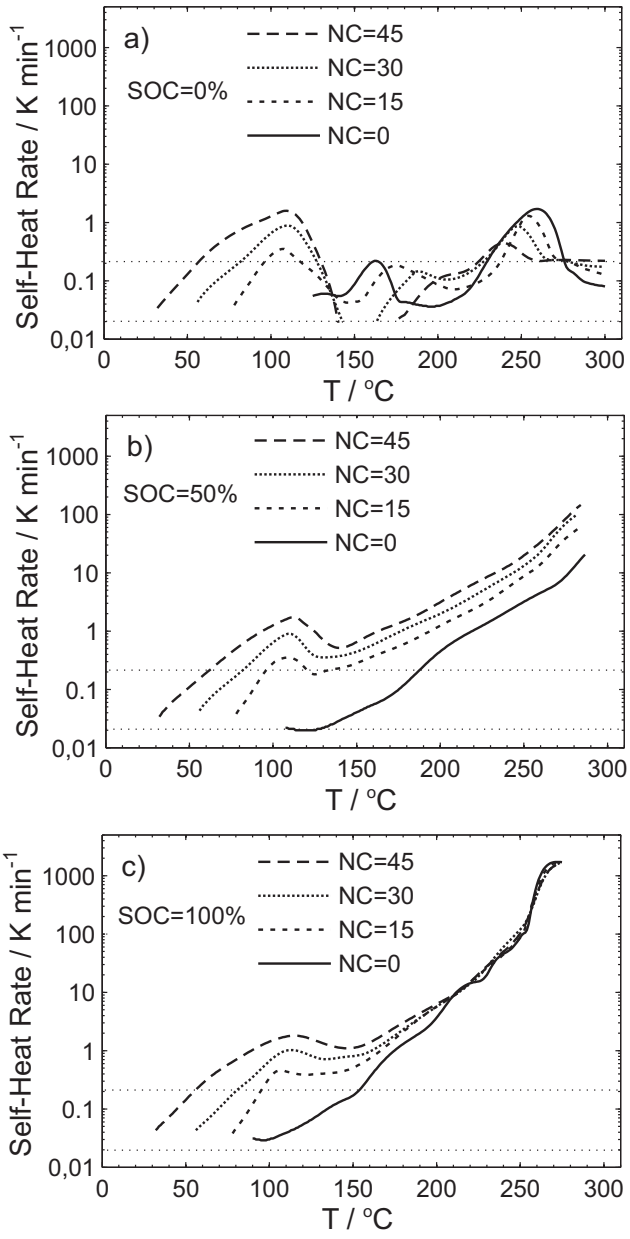

Figure 2. Results of ARC-HWS calorimetric measuring for cells 18650 (NCM/Graphite) with number of charge/discharge cycles NC = 0, 15, 30 and 45 (at the temperature 0°C), while the cells are charged to 0% SOC (a), 50% SOC (b) and 100% SOC (c). The dashed lines are indicative of the initial temperature of the exothermic reactions (at SHR = 0.02 K min^{-1}) and the thermal runaway temperature at SHR = 0.2 K min^{-1}.

Table I. Experimental parameters of first group of exothermic reactions.

Number of charge/discharge cycles	0	15	30	45
Temperature range of exothermic reactions of first group (°C)	0	78-105	56-110	32-116
Energy of exothermic reactions of first group[a] (kJ)	0	1.08	2.14	3.29

[a]The relative error in the data is 2.7%.

reaction is initiated by way of reduction of carbonates from an anode by means of LI^+ and e^-. Nevertheless, no experimental proves in support of this hypothesis are given by the authors. They make reference to investigations of electrolyte thermal degradation (based on EC/DMC) made in the paper.[31] However this hypothesis raises doubts.

Firstly, in the paper,[31] it was shown that the exothermic reactions of electrolyte thermal degradation on an anode emerge in the temperature range from 120 to 270°C, while the exothermic reactions of the first group (Fig. 2) appear in the temperature range from 32 to 116°C, i.e. at much lower temperature range.

Secondly, in the work,[31] it was shown that the exothermic reactions of the electrolyte thermal degradation on an anode depend much on degree of delithiation of an anode, i.e. on SOC. In particular, on a completely delithiated anode, these exothermic reactions are absent whatsoever. Meanwhile, the exothermic reactions of the first group do not depend on SOC at all (Fig. 2).

It is worth to observe that an amount of released energy (in any exothermic reactions, the active participant of which is lithium) must depend heavily on the lithium amount in an anode, i.e. on SOC. Notably that this is true for both lithium intercalated into graphite[31] and lithium precipitated (in the course of cells cycling) on an anode surface.

Unambiguously, the independence of the first group of the exothermic reactions from SOC is indicative of the fact that the lithium is not a participant of these exothermic reactions.

The second property of the first group of the exothermic reactions is the fact that their intensity grows in proportion to a number of cells charge/discharge cycles (Fig. 2). Hence, the active reagents of the first group of the exothermic reactions are accumulated in an anode in the course of the cells cycling.

As a function of a number of cells charge/discharge cycles, the energy released by the exothermic reactions of the first group can be calculated in the adiabatic mode using the following formula:

$$H = \int_{T1}^{T2} c_p dT, \qquad [1]$$

where c_p – specific heating capacity of a cell; T1 and T2 – adiabatic temperature range of beginning and end of exothermic reactions.

The specific heating capacity of a cell was measured in the ARC-calorimeter for new and completely discharged cells in the temperature range from 30°C to 120°C. As it is seen on Fig. 3a, in the case of new discharged cells, the exothermic reactions start at temperature values higher than 125°C; thus they are not able to influence a value of a cell specific heating capacity. For calculating of the specific heating capacity of a cell, we obtained the expression

$$c_p = 35.956 + 0.044 \cdot T(J/^\circ C)\,. \qquad [2]$$

Temperature ranges of the first group of the exothermic reactions do not depend on SOC (Table I and Fig. 2). Hence, also values of the energy released by the exothermic reactions of the first group do not depend on SOC. However, they depend heavily on a number of cell charge/discharge cycles (Table I). In the Table I, it is seen that the energy released as a result of the exothermic reactions of the first group increases with a number growth of cell charge/discharge cycles. Thus active reagents of these reactions are accumulated in an anode in the process of cell cycling.

The third property of the first group of the exothermic reactions is the intensive gas release in the process of these reactions. Indirectly, this can be determined in the ARC experiments in activation of the current interrupt device. At low values of pressure in a cell, a current is able to run through a cell. In a case of higher pressure values in a cell, the current interrupt device is activated; as a result, the current is interrupted and the voltage falls. For cells with NC = 0 (which have no exothermic reactions of the first group, Fig. 2), the current interrupt device is activated at temperature values approximately 115–150°C depending on SOC, Fig. 3c. For cells with NC = 45 (at which the exothermic reactions of the first group do take place, Fig. 2), the current interrupt device is activated approximately at the temperature 75–85°C regardless of SOC, Fig. 3c. The activation of the current

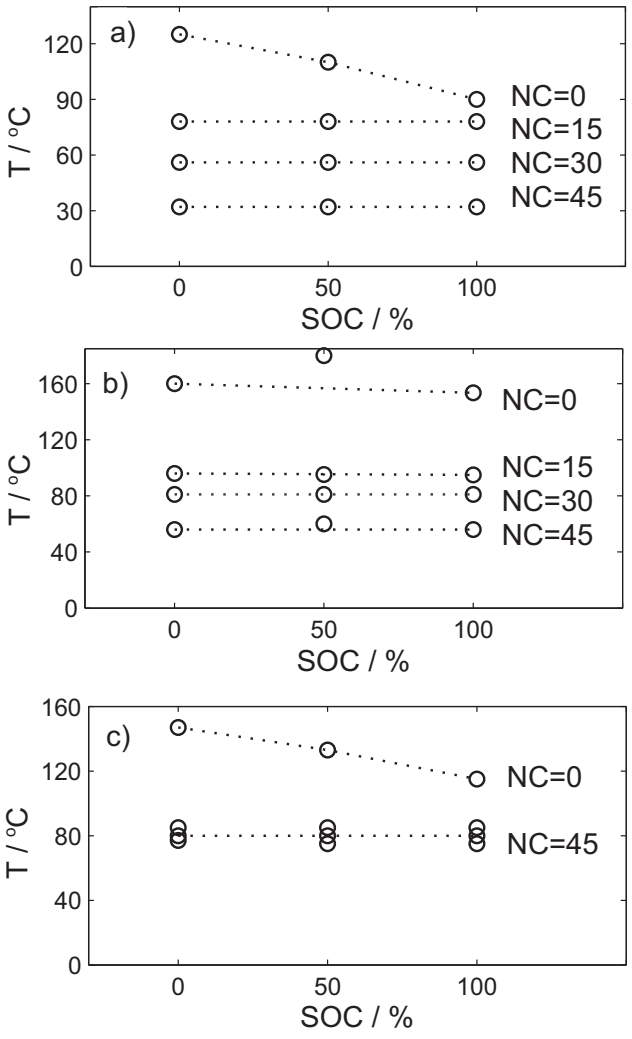

Figure 3. Parameters changing for Self-Heating Rate of cells during ARC-HWS calorimetric measuring following an initiation of the thermal runaway exothermic reactions: a) temperature of exothermic reaction initiation (at SHR = 0.02 K min^{-1}), b) temperature of thermal runaway at SHR = 0.2 K min^{-1}, c) temperature of current interrupt device activation.

interrupt device at lower temperature values is indicative of release of a great amount of gas released as a result of these reactions.

In our previous papers,[32–34] in the frame of the thermal runaway mechanism investigation in alkaline batteries, it was proven by experiments that the thermal runaway in these batteries is not connected with an acceleration of standard electrochemical reactions (batteries' charge and decomposition of electrolyte) due to their self-heating up as it is thought traditionally.[35] In these papers, it was proven by experiments that in fact, the thermal runaway in alkaline batteries is connected with emergence of a new powerful exothermic reaction of recombination of atomic hydrogen accumulated in electrodes of the batteries during their long operation, i.e.

$$H + H \rightarrow H_2 \uparrow \qquad [3]$$

The reaction (Eq. 3) is a powerful exothermic reaction with heat emission 436 kJ/mole (hydrogen).[36] This heat emission is more intensive than in the reaction of hydrogen burning in oxygen and is equal to 285.8 kJ/mole (hydrogen).[37]

The reaction (Eq. 3) starts in line with the electrochemical mechanism:[32]

$$\begin{aligned} &H_2O + H_{ads} + e^- \rightarrow H_2 \uparrow + OH^- \text{ (anode)} \\ &H_{ads} + OH^- \rightarrow H_2O + e^- \text{ (cathode)}. \end{aligned} \qquad [4]$$

After electrodes heating up in the spot of the would-be thermal runaway,[38,39] the reaction continues in line with both electrochemical mechanism (Eq. 4) and pure chemical mechanism (Eq. 3) due to hydrogen atoms diffusion to electrodes surface and their recombination.

In the papers,[40–42] it was shown that during a long operation of nickel-cadmium batteries into their electrodes, a great deal of hydrogen is accumulated. The hydrogen accumulation takes place during batteries charging. During charging (performed in accordance with service instruction), the batteries are recharged 1.5 times more in comparison with their nominal capacity. Upon that, an electrolyte is decomposed into hydrogen and oxygen. The experiments showed[39–42] that oxygen escapes from batteries, while as for hydrogen, partially it escapes and partially is accumulated in the electrodes. This is connected with the fact that hydrogen has a very high diffusional penetrability as compared to all other gases. For example, at the temperature 20°C, the coefficient of hydrogen diffusion in nickel is approximately 10^{10} times larger than the nitrogen or oxygen diffusion coefficients.[43] That is why at electrolyte dissociation in batteries, only hydrogen is accumulated in electrodes, while oxygen escapes to atmosphere.[39-42] Hydrogen is accumulated either in ceramic-metal matrix of electrodes (in the case of sintered electrodes)[40–42] or in graphite as it is an electroconductive addition in pocket and pressed electrodes.[44,45] For example, in a battery KSX-25 (25Ah) after five years of operation, 800 liters of hydrogen is accumulated.[34] The hydrogen intercalates and is present inside of sintered matrix of electrodes or graphite in atomic form.[40,43,46]

Experiments showed that in a case of thermal runaway from a battery KSX-25, approximately 351 liters of vapor-gas mixture escapes: 63 liters of vapor and 288 liters of gas. The vapor amount is approximately equal to electrolyte amount being in a battery before a thermal runaway; meanwhile the gas is represented mainly by hydrogen (94–97%, 270–280 liters).[34] The rest of the gas was oxygen and as for other gases, there were less than 0.5% of them (products of separator burning). Calorimetric measuring showed that in a battery KSX-25, thermal runaway results in a release of approximately 5012 kJ of heat.[32] This value conforms fully to the exothermic reaction (Eq. 3) in accordance with the released hydrogen amount.

Approximately similar processes take place in the lithium-ion cells, too, and it happens in a beginning of a thermal runaway.

Firstly, in the paper,[47] it was shown that as a result of a thermal runaway in commercial lithium-ion cells with geometrical format 18650 (1.5 Ah, NCM/Graphite), 3.338 liters of gas mixture escapes. Besides, with aid of a gas chromatograph, there was found the gas mixture percentage composition: the gas mixture contains 1.028 liters of hydrogen; 1.375 liters of CO_2; 0.043 liters of CO; 0.023 liters of CH_4 and 0.027 liters of C_2H_4. Thus, at thermal runaway from lithium-ion cells, a considerable amount of hydrogen escapes, just as in alkaline batteries.[48]

Secondly, in the paper,[49] it was shown that at cycling of lithium-ion cells on an anode, the following gases release: H_2, CO and C_2H_4. At the same time on a cathode, the gases CO and CO_2 release. C_2H_4 release is connected with forming of SEI layer. In the same paper, it was shown that other gases release is connected with electrolyte decomposition as it continues constantly during cells cycling. These gases release starts in a cell at charge voltage more than 4.0 V. Hence in investigated by us lithium-ion cells during their charging, obligatory, hydrogen must release on anode (just as in alkaline batteries).

In the papers,[42,45] it was shown that in a case of hydrogen release on a pocket anode, obligatory, it is accumulated in graphite, which is an elecroconductive addition in these electrodes. Notably that hydrogen not only is adsorbed by graphite but also penetrates inside of the graphite, where it is contained in atomic state.[43,46]

It is worth to be mentioned that the investigated lithium-ion cells are not fully hermetical. In order to check this fact, we measured a cell internal pressure by standard method in frame of ARC- calorimetry[50] at different temperatures in the range from the room temperature 25°C to the temperature of reactions beginning of the thermal runaway, Fig. 3b at NC = 0. Upon that, a pressure in a cell can grow almost to 4 bar before reactions initiation of the exothermic decomposition. After that, if to stop the experiment, during 1–2 hours, the pressure in the cell decreases trice. Thus, sealing rings in the cell are able to pass gas at a high enough pressure inside of the cell. Hence the gas escaping in lithium-ion cells during cycling can leave the cells, while the released hydrogen – in virtue of its high diffusional penetrability – can be partially accumulated in graphite of anode and partially leave the cell (just as in alkaline vented batteries).[34]

That is why it is possible to suppose that also in lithium-ion cells, while releasing at the anode, hydrogen is accumulated in graphite and exerts its influence to a process of thermal runaway in these cells. With purpose of this hypothesis checking, we conducted additional experiments in ARC calorimeter for finding out of hydrogen possible accumulation in anode.

The additional ARC-calorimetric measuring was conducted by us based on three groups of cells with numbers of charge/discharge cycles NC = 15, 30 and 45 (at temperature T = 0°C). In common with the experiments shown in Fig. 2, for these groups of cells, the initial temperature was chosen 68°C, 46°C and 27°C respectively. The final temperature was determined in accordance with the final temperature of the first group of the exothermic reactions 105°C, 110°C and 116°C (Table I) respectively. Besides, in each group of cells, measuring was conducted for cells with SOC = 0%, 50% and 100%. Thus, the measuring was conducted for nine groups of cells. The rest parameters for these experiments were the same as in experiments shown in Fig. 2.

A cell was placed inside of sealed canister, which was placed then in a calorimeter chamber and connected to a system of gas collection SSS (single sample system). As we were interested with the gas accumulated in the anode, before cell placing to the sealed canister, a pressure-sealing disk of a current interrupt device of the cell (close to its positive terminal) was punched through by a piercer. The cell punching and placing into the sealed canister was performed in a glove box in atmosphere of argon ($O_2 < 0.1$ ppm, $H_2O < 0.1$ ppm). The cell punching allowed getting rid of residual gases accumulated inside of the cell during its cycling and ensured a free gas escape from the cell during the experiments. In the system SSS, a standard gas collection vessel was replaced by elastic metering container. Notably that at first, the gas escaping from the system SSS passed through a standard coil cooler and then came to the metering container. As a result of passing through the standard coil cooler, the gas cooled down to the room temperature. This allowed separating the gas from vapors of the electrolyte. Based on change of volume of the elastic metering container (with pressure inside of it equal to atmospheric pressure), it was possible to find out the released gas amount within the accuracy of 0.1 ml.

Table II. Gas release from cells as applied to first group of exothermic reactions.[a]

Number of charge/discharge cycles	15			30			45		
SOC (%)	0	50	100	0	50	100	0	50	100
Amount of gas released (ml)	57.3	56.5	57.6	113.5	114.9	113.1	170.9	173.5	171.9
Amount of H_2 released (ml)	56.8	56.0	57.2	112.5	114.1	112.2	169.5	172.1	171.0
Energy of exothermic reaction (Eq. 3) (kJ)	1.11	1.09	1.11	2.19	2.22	2.18	3.30	3.35	3.33

[a]The relative error in the data in Table II is 3%.

A presence of any non-inert gases in the experimental system can lead to changes of real composition of gases released from a cell during experiments. In order to exclude a presence of any other gases in the system except for inert argon, all parts of the described metering system were assembled in the glove box in the atmosphere of argon.

After reaching the final temperature in the ARC-calorimeter, the released gas from the cell was directed (with aid of the system SSS) into the metering container; then, the system was cooled down quickly by compressed air. In order to guarantee reproducibility of data, the entire measuring was performed not less than three times for each group of cells. The measuring results are represented in the Table II.

The gas mixture from the metering container was analyzed with aid of a gas chromatograph (GC, Agilent Technologies 3000 Micro GC, two columns, Mol Sieve and PLOTU). A thermal conductivity detector was used to detect permanent gases. The GC was calibrated for H_2, O_2, N_2, CO, CO_2, CH_4, C_2H_2, C_2H_4 and C_2H_6. Argon was used as a carrier gas. The conducted measuring showed that the obtained gas from a cells consisted of hydrogen (more than 99%), while the other gases (CO_2, CO, CH_4 and C_2H_4) accounted for less than 1%.

Based on the known amount of the gas obtained from the cell and the hydrogen percentage, an amount of obtained hydrogen was computed for each conducted experiment (Table II). Besides, for the found amount of hydrogen, there was calculated a heat amount released by a cell on expense of the powerful exothermic reaction (Eq. 3) of recombination of atomic hydrogen accumulated in anode graphite (Table II).

Separately, the direct experimental testing was accomplished of hydrogen accumulation in anode graphite in the course of cells cycling (NC = 15,30,45). With this purpose, the cells were discharged in full (SOC = 0%). The cells were opened in a glove box in atmosphere of argon (O_2 < 0.1 ppm, H_2O < 0.1 ppm) with a cutting tool from both sides. The jelly roll was removed from its case and the individual parts (outer separator, anode, inner separator, and cathode) were separated. Electrodes were washed twice with dimethyl carbonate (DMC, anhydrous, ≥ 99%) to remove the conductive salt and other electrolyte residues. The electrodes were dried afterwards in the glove box. After this with the anodes, experiments were conducted similar to the experiments represented in the Table II. The obtained amounts of the hydrogen released from the anodes coincided with the results given in the Table II with the relative error 6%. Thus straightforwardly, this experimental research proves that in the course of cells cycling in anode graphite, hydrogen is accumulated.

From analysis of the Table II, it is possible to make the following conclusions. Firstly, a hydrogen amount released from a cell does not depend on SOC but heavily depend on a number of charge/discharge cycles. Hence, hydrogen is accumulated in a cell during its cycling. Secondly, an amount of heat released by a cell due to the exothermic reaction of recombination of atomic hydrogen accumulated in anode graphite (Table II) is equal to a heat amount (in limits of experimental error) found by us based on thermal effects observed for the first group of the exothermic reactions (Table I). Thus, the conducted experimental investigation proves that the first group of the exothermic reactions represents only one powerful exothermic reaction, namely one of recombination of atomic hydrogen accumulated in anode graphite.

Conclusions

The conducted experiments in ARC-calorimeter show that during cycling of lithium-ion cells in anode graphite, there is accumulated hydrogen, which exists inside of graphite in atomic form. Upon cell heating up to the temperature, at which mass release starts of atomic hydrogen from graphite, the powerful exothermic reaction of recombination of atomic hydrogen with heat release 436 kJ/mole starts. An amount of energy released in this reaction is determined only by amount of accumulated hydrogen (i.e. by a number of charge/discharge cycles) and does not depend on SOC in accordance with the experimental data (Fig. 2 and Table II). As with a hydrogen amount growth in graphite, its activation energy must decrease, so also an initial temperature of the exothermic reaction of the thermal runaway must decreases; Fig. 3a.

Thus, the first exothermic reaction at a thermal runaway in aged cells is the exothermic reaction of recombination of atomic hydrogen accumulated in anode graphite. It increases considerably a heat release in a beginning of a thermal runaway. Afterwards in a case of cell sufficient heating up, the exothermic reactions start in connection with SEI layer destruction and its restoration due to electrolyte reduction.[11,27,28] Upon reaching the temperature of initiation of oxygen release from cathode, approximately at $T_{ox} \approx 200–250^{\circ}C$, the exothermic reactions start of electrolyte burning on a cathode. The latter reactions are dominant in a course of a thermal runaway of lithium-ion cells.[5]

ORCID

N. E. Galushkin https://orcid.org/0000-0002-1613-8659

References

1. G. E. Blomgren, *J. Electrochem. Soc.*, **164**, A5019 (2017).
2. X. Feng, M. Fang, X. He, M. Ouyang, L. Lu, H. Wang, and M. Zhang, *J. Power Sources*, **255**, 294 (2014).
3. H. U. Escobar-Hernandez, R. M. Gustafson, M. I. Papadaki, S. Sachdeva, and M. S. Mannana, *J. Electrochem. Soc.*, **163**, A2691 (2016).
4. S. U. Kim, P. Albertus, D. Cook, C. W. Monroe, and J. Christensen, *J. Power Sources*, **268**, 625 (2014).
5. D. H. Doughty and E. P. Roth, *Electrochem. Soc. Interface*, **21**, 37 (2012).
6. L. Somerville, J. Bareno, S. Trask, P. Jennings, A. McGordon, C. Lyness, and I. Bloom, *J. Power Sources*, **335**, 189 (2016).
7. C. H. Lee, S. J. Bae, and M. Jang, *J. Power Sources*, **293**, 498 (2015).
8. S. Abada, G. Marlair, A. Lecocq, M. Petit, V. Sauvant-Moynot, and F. Huet, *J. Power Sources*, **306**, 178 (2016).
9. A. M. Andersson, K. Edstrom, and J. O. Thomas, *J. Power Sources*, **81–82**, 8 (1999).
10. H. H. Lee, C. C. Wan, and Y. Y. Wang, *J. Electrochem. Soc.*, **151**, A542 (2004).
11. P. Biensan, B. Simon, J. Peres, A. de Guibert, M. Broussely, J. Bodet, and F. Perton, *J. Power Sources*, **81–82**, 906 (1999).
12. V. Kraft, M. Grützke, W. Weber, J. Menzel, S. Wiemers-Meyer, M. Winter, and S. Nowak, *J. Chromatogr. A*, **1409**, 201 (2015).
13. M. Grützke, V. Kraft, B. Hoffmann, S. Klamor, J. Diekmann, A. Kwade, M. Winter, and S. Nowak, *J. Power Sources*, **273**, 83 (2015).
14. P. Niehoff, E. Kraemer, and M. Winter, *J. Electroanal. Chem.*, **707**, 110 (2013).
15. P. Roder, B. Stiaszny, J. C. Ziegler, N. Baba, P. Lagaly, and H.-D. Wiemhofer, *J. Power Sources*, **268**, 315 (2014).
16. M. Fleischhammer, T. Waldmann, G. Bisle, B.-I. Hogg, and M. Wohlfahrt-Mehrens, *J. Power Sources*, **274**, 432 (2015).
17. A. Friesen, F. Horsthemke, X. Monnighoff, G. Brunklaus, R. Krafft, M. Borner, T. Risthaus, M. Winter, and F. M. Schappacher, *J. Power Sources*, **334**, 1 (2016).
18. A. Friesen, C. Schultz, G. Brunklaus, U. Rodehorst, A. Wilken, J. Haetge, M. Winter, and F. Schappacher, *ECS Trans.*, **69**, 89 (2015).
19. S. Krueger, R. Kloepsch, J. Li, S. Nowak, S. Passerini, and M. Winter, *J. Electrochem. Soc.*, **160**, A542 (2013).

20. Z. Li, J. Huang, B. Yann Liaw, V. Metzler, and J. Zhang, *J. Power Sources*, **254**, 168 (2014).
21. M.-H. Ryou, Y. M. Lee, Y. Lee, M. Winter, and P. Bieker, *Adv. Funct. Mater*, **25**, 834 (2015).
22. M. Winter, *Z. Phys. Chem.*, **223**, 1395 (2009).
23. C.-K. Huang, J. S. Sakamoto, J. Wolfenstine, and S. Surampudi, *J. Electrochem. Soc.*, **147**, 2893 (2000).
24. J. Vetter, P. Novak, M. R. Wagner, C. Veit, K.-C. Moller, J. O. Besenhard, M. Winter, M. Wohlfahrt-Mehrens, C. Vogler, and A. Hammouche, *J. Power Sources*, **147**, 269 (2005).
25. D. Liu, J. Pang, J. Zhou, Y. Peng, and M. Pecht, *Microelectron. Reliab*, **53**, 832 (2013).
26. R. Hein, P. R. Kleindorfer, and S. Spinler, *Technol. Forecase. Soc.*, **79**, 1654 (2012).
27. H. Park, T. Yoon, Y. Kim, J. G. Lee, J. Kim, H.-s. Kim, J. H. Ryu, J. J. Kim, and S. M. Oh, *J. Electrochem. Soc.*, **162**, A892 (2015).
28. A. W. Golubkov, S. Scheikl, R. Planteu, G. Voitic, H. Wiltsche, C. Stangl, G. Fauler, A. Thaler, and V. Hackerb, *RSC Adv.*, **5**, 57171 (2015).
29. H. Maleki and J. N. Howard, *J. Power Sources*, **137**, 117 (2004).
30. D. D. MacNeil, Z. Lu, Z. Chen, and J. R. Dahn, *J. Power Sources*, **108**, 8 (2002).
31. G. Gachot, S. Grugeon, G. G. Eshetu, D. Mathiron, P. Ribiere, M. Armand, and S. Laruelle, *Electrochim. Acta*, **83**, 402 (2012).
32. N. E. Galushkin, N. N. Yazvinskaya, and D. N. Galushkin, *J. Electrochem. Soc.*, **162**, A749 (2015).
33. N. E. Galushkin, N. N. Yazvinskaya, and D. N. Galushkin, *J. Electrochem. Soc.*, **162**, A2044 (2015).
34. D. N. Galushkin, N. N. Yazvinskaya, and N. E. Galushkin, *J. Power Sources*, **177**, 610 (2008).
35. Y. Guo, in *Encyclopedia of Electrochemical Power Sources*, Vol. **4**, J. Garche, Editor, p. 241, Elsevier, Amsterdam (2009).
36. S. J. Blanksby and G. B. Ellison, *Acc. Chem. Res.*, **36**, 255 (2003).
37. *The Hydrogen Economy: Opportunities, Costs, Barriers, and R&D Needs*, p.240, National Academies Press., Washington (2004).
38. N. N. Yazvinskaya, N. E. Galushkin, D. N. Galushkin, and I. A. Galushkina, *Int. J. Electrochem. Sci.*, **11**, 10287 (2016).
39. N. E. Galushkin, N. N. Yazvinskaya, D. N. Galushkin, and I. A. Galushkina, *J. Electrochem. Soc.*, **161**, A1360 (2014).
40. N. E. Galushkin, N. N. Yazvinskaya, D. N. Galushkin, and I. A Galushkina, *Int. J. Hydrogen Energy*, **39**, 18962 (2014).
41. N. E. Galushkin, N. N. Yazvinskaya, and D. N. Galushkin, *ECS Electrochemistry Letters*, **2**, A1 (2013).
42. N. N. Yazvinskaya, N. E. Galushkin, D. N. Galushkin, and I. A. Galushkina, *Int. J. Electrochem. Sci.*, **11**, 7843 (2016).
43. D. P. Broom, *Hydrogen Storage Materials*, p.7, Springer, London, (2011).
44. N. E. Galushkin, N. N. Yazvinskaya, D. N. Galushkin, and I. A. Galushkina, *Int. J. Electrochem. Sci.*, **10**, 6645 (2015).
45. N. E. Galushkin, N. N. Yazvinskaya, and D. N. Galushkin, *J. Electrochem. Soc.*, **164**, A2555 (2017).
46. N. N. Yazvinskaya, N. E. Galushkin, D. N. Galushkin, and I. A. Galushkina, *Int. J. Electrochem. Sci.*, **12**, 2791 (2017).
47. A. W. Golubkov, D. Fuchs, J. Wagner, H. Wiltsche, C. Stangl, G. Fauler, G. Voitic, A. Thalera, and V. Hackere, *RSC Adv.*, **4**, 3633 (2014).
48. N. E. Galushkin, N. N. Yazvinskaya, D. N. Galushkin, and I. A. Galushkina, *Int. J. Electrochem. Sci.*, **9**, 3022 (2014).
49. M. Metzger, B. Strehle, S. Solchenbach, and H. A. Gasteiger, *J. Electrochem. Soc.*, **163**, A798 (2016).
50. B. Lei, W. Zhao, C. Ziebert, N. Uhlmann, M. Rohde, and H. J. Seifert, *Batteries*, **3**, 1 (2017).